Vacuum 84 (2010) 1199–1203

Contents lists available at ScienceDirect

Vacuum

journal homepage: www.elsevier.com/locate/vacuum

Characterization on pulsed laser deposited nanocrystalline ZnO thin films

S. Venkatachalam [a,*], Yoshinori Kanno [b,*], S. Velumani [c]

[a] National Institute of Advanced Industrial Science and Technology (AIST), 4-2-1 Nigatake, Miyagino-ku, Sendai 983-8551, Japan
[b] Advanced Institute of Industrial Technology, Tokyo Metropolitan University, Shinagawa, Tokyo 140-0011, Japan
[c] Department of Electrical Engineering (SEES), CINVESTAV-IPN, Zacatenco, D.F., 07360, Mexico

Keywords:
PLD
Thin films
XPS
AFM
Optical transmittance
XRD

A B S T R A C T

Nanocrystalline zinc oxide thin films were deposited on glass and silicon substrates by using pulsed laser deposition at different laser energy densities (1.5, 2, and 3 J/cm^2). The film thickness, surface roughness, composition, optical and structural properties of the deposited films were studied using an α-step surface profilometer, atomic force microscopy (AFM), X-ray photoelectron spectroscopy (XPS), optical transmittance, and X-ray diffraction (XRD), respectively. The film thickness was calculated as 244 nm. AFM analysis shows that the root-mean-square roughness increases with increasing laser energy density. XPS analysis shows that the interaction of zinc with oxygen atoms is greatly increased at high laser energy density. In the optical transmittance spectra, a shift of the absorption edge towards higher wavelength region confirms that the optical band gap increases with an increase in laser energy density. The particle size of the deposited films was measured by XRD, it is found to be in the range from 7.87 to 11.81 nm. It reveals that the particle size increases with an increase in laser energy density.

1. Introduction

In recent years, research and development has been focused on the preparation and characterization of optoelectronic devices such as gas sensors and photodiodes [1]. The II-VI compound semiconductors are a very suitable candidate for these applications. In the II-VI compound semiconductors, ZnO play an important role for gas sensor applications. The basic principle of the gas sensor is that the electrical conductivity of metal (Zn) oxide semiconductors usually changes when exposed to certain gases. In particular, n-ZnO has extensively been used for detecting reducing gases such as CO, CH4, and alcohol [2,3]. In order to improve the gas sensing properties, materials preparation, and characterization plays a main role either by changing the technology from micro into nano [4] or by adding catalysts to the ZnO [5], because the sensing mechanism of semiconducting oxide gas sensors is mainly based on the surface reaction of semiconducting oxides. In particular, a gas sensor based on ZnO nanoparticles shows good sensing properties due to its high surface-volume ratio. A broad variety of techniques have been used for the deposition of nanocrystalline ZnO films, such as metallorganic chemical vapour deposition [6], sol-gel method [7], hydrothermal growth [8], thermal evaporation [9] and pulsed laser deposition [10]. Among these techniques, pulsed laser deposition is an important promising technique to prepare nanocystalline ZnO films at room temperature. In this paper, we study the composition, surface morphology, optical, and structural properties of nanocrystalline ZnO thin films by using X-ray photoelectron spectroscopy, atomic force microscopy, optical transmittance, and X-ray diffraction.

2. Experimental details

Nanocrystalline ZnO thin films were deposited onto glass and silicon (100) substrates by using pulsed laser deposition under a vacuum of 4×10^{-5} mbar at 303 K. Oxygen pressure in the deposition chamber was maintained at 0.025 mbar during the film deposition. Fig. 1 shows the experimental set-up of the pulsed laser deposition system. The distance between the substrate and target was maintained at 35 mm. Rotation of the substrate and target was maintained at 20 and 4 rpm, respectively during laser ablation. A KrF laser with a wavelength and pulse repetition rate of 248 nm and 10 Hz, respectively was used for the ablation of ZnO targets. The laser fluence was varied from 1.5 to 3 J/cm^2. High purity ZnO (99.99%, Ishizu Pharmaceutical Co., Ltd., Osaka, Japan) powder was used to prepare the ZnO targets. We used polyvinyl alcohol (PVA) as a binder solution to prepare these ZnO targets. First we thoroughly mixed the ZnO powder with binder solution for about 1 h. Finally ZnO pellets were obtained by the uniaxial pressing at 300 kg/cm^2 and then the prepared ZnO pellet was sintered at 1200 °C for 3 h in

* Corresponding authors. Tel.: +81 3 3472 7831; fax:+81 3 3472 2790.
E-mail addresses: svchalam23@yahoo.co.in (S. Venkatachalam), fujikurosawakabuki@yahoo.co.jp (Y. Kanno).

0042-207X/$ – see front matter © 2009 Elsevier Ltd. All rights reserved.
doi:10.1016/j.vacuum.2009.10.025

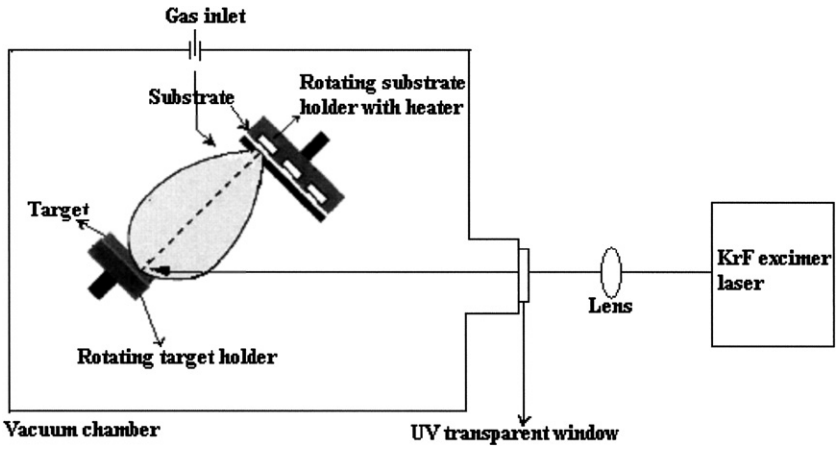

Fig. 1. Experimental set-up of pulsed laser deposition.

order to densify the targets. Compositional analysis of the ZnO films was performed using X-ray photoelectron spectroscopy (XPS). Structural properties of the deposited films were studied by using X-ray diffraction (XRD) with Ni – filtered Cu Kα radiation [Model-RINT 2000; 52 kV/120 mA; $\lambda = 1.54056$ Å]. Atomic force microscopy (AFM) (SPI3800/SPA300, Seiko Instruments Inc.) was used to study the surface roughness of the deposited films. Optical transmittance spectra of the deposited films were recorded by using UV-Vis-NIR spectrophometer in the range 300–800 nm.

3. Results and discussion

3.1. Composition and surface analysis

The film thickness was measured by using an α-step surface profilometer. Thickness of the deposited films was calculated as 244 nm. Wide scan X-ray photoelectron spectra of nanocrystalline ZnO films deposited on silicon substrates at different laser energy densities (1.5, 2, and 3 J/cm^2) are shown in Fig. 2. The peak positions of Zn2p, Ols, Cls, and Zn LMM for the films deposited at 1.5 J/cm^2 are positioned at 1021.06, 531.67, 284.94, and 266.23 eV, respectively. Narrow scan XPS spectra of Zn peaks at different energy density is shown in Fig. 3(a). The peak position of Zn2p3/2 for ZnO films deposited at 1.5 J/cm^2 is positioned at 1021.06 eV. It confirms the oxygen deficiency of the deposited films. The peak position of Zn2p$_{3/2}$ shifts towards the low energy side with the increase of laser energy density. This is due to the fact that the laser energy density for nanocrystalline ZnO films deposited at 1.5 J/cm^2 is not sufficient to bind the Zn atom with oxygen [11]. The incorporation of Zn with oxygen is greatly increased at 3 J/cm^2. In Fig. 2, we can see a peak at 266.23 eV; it corresponds to Zn LMM. The peak intensity of Zn LMM decreases with an increase in laser energy density. This is attributed to the fact that the content of Zn free state decreased considerably at high laser energy density. Fig. 3(b) shows the narrow scan XPS spectra of oxygen peak at different laser

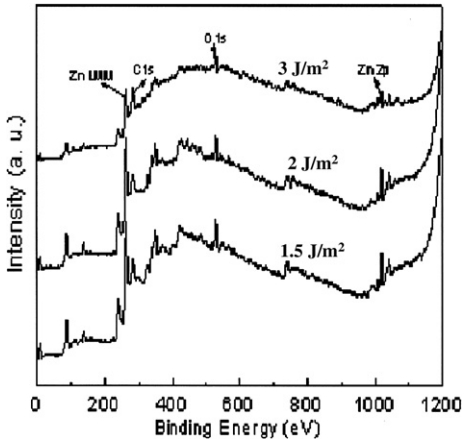

Fig. 2. Wide scans XPS spectra for nanocrystalline ZnO thin films deposited at 1.5, 2 and 3 J/cm^2.

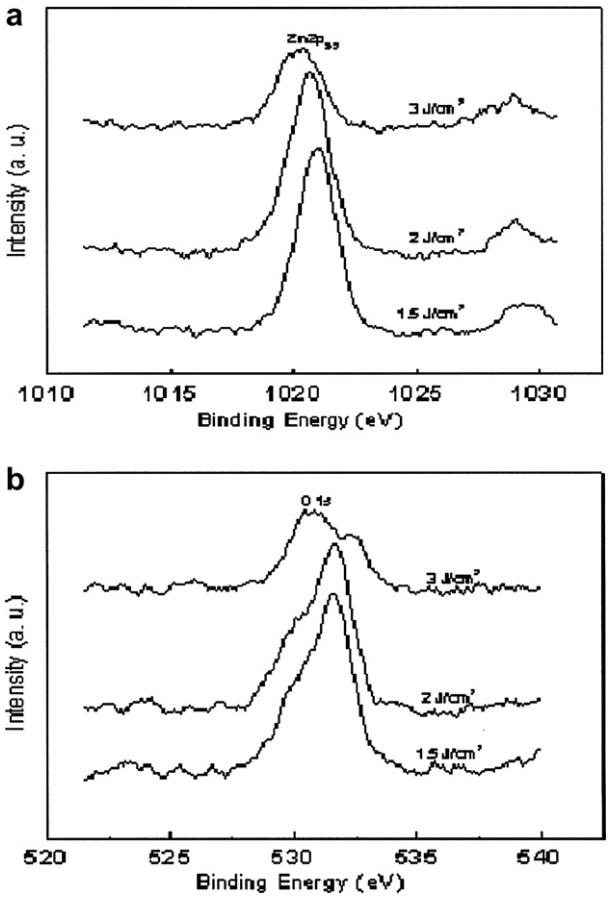

Fig. 3. (a, b) Narrow scans XPS spectra of Zn and O peaks deposited at 1.5,2 and 3 J/cm^2.

Table 1
List of composition, surface roughness and optical parameters of nanocrystalline ZnO thin films.

Deposition parameters	Atomic ratio (O/Zn)	Surface roughness (nm)		Optical band (eV) gap
		Mean roughness	RMS roughness	
1.5 J/cm^2	1.668	10.63	14.54	3.314
2 J/cm^2	1.702	11.93	16.10	3.362
3 J/cm^2	1.740	19.76	25.34	3.391

energy densities. We can observe only one peak for the films deposited at 1.5 and 2 J/cm^2, which are located at around 531.61 and 531.73 eV, respectively. It is attributed that the film deposited at low laser energy density is in oxygen enriched state. This may be for the following two reasons: First is the presence of loosely bound oxygen due to surface contamination or OH group and the second is the presence of a non-stoichiometric nanocrystalline ZnO film. But the Ols peak for the film deposited at 3 J/cm^2 is splitting into two components. One is located at 532.37 eV and other one is located at 530.85 eV. It is attributed that the peak position at 530.85 eV corresponds to O^{2-} ions on the wurtzite structure of hexagonal Zn^{2+} ion array, surrounded by Zn atoms with their full complement of nearest neighbor O^{2-} ions [12]. The high binding energy component located at 532.37 eV is attributed to the either the presence of loosely bound oxygen on the surface of the films or belongs to hydrated oxides, which might be incorporated from deposition chamber [11]. Stoichiometry behaviour of the films is given Table 1. It shows that the O/Zn ratio increases with an increase in laser energy density and confirms that the increase of crystallite size with an increase in laser energy density leads to an increase of O/Zn atomic ratio.

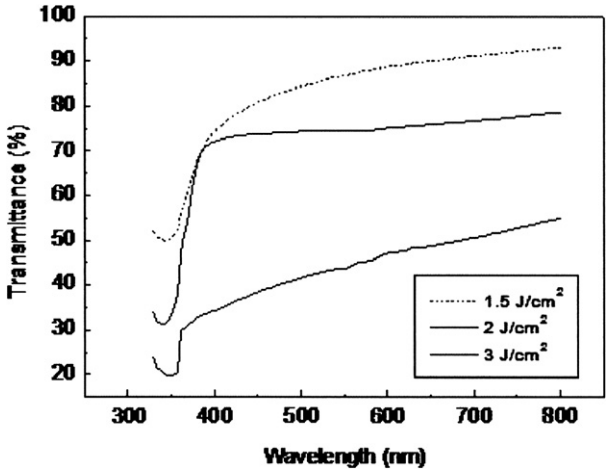

Fig. 5. Transmittance spectra for nanocrystalline ZnO thin films deposited at different laser energy density (1.5, 2, and 3 J/cm^2).

Fig. 4(a–c) show the two dimensional (1 × 1 μm) AFM images of nanocrystalline ZnO thin films deposited on silicon substrates at

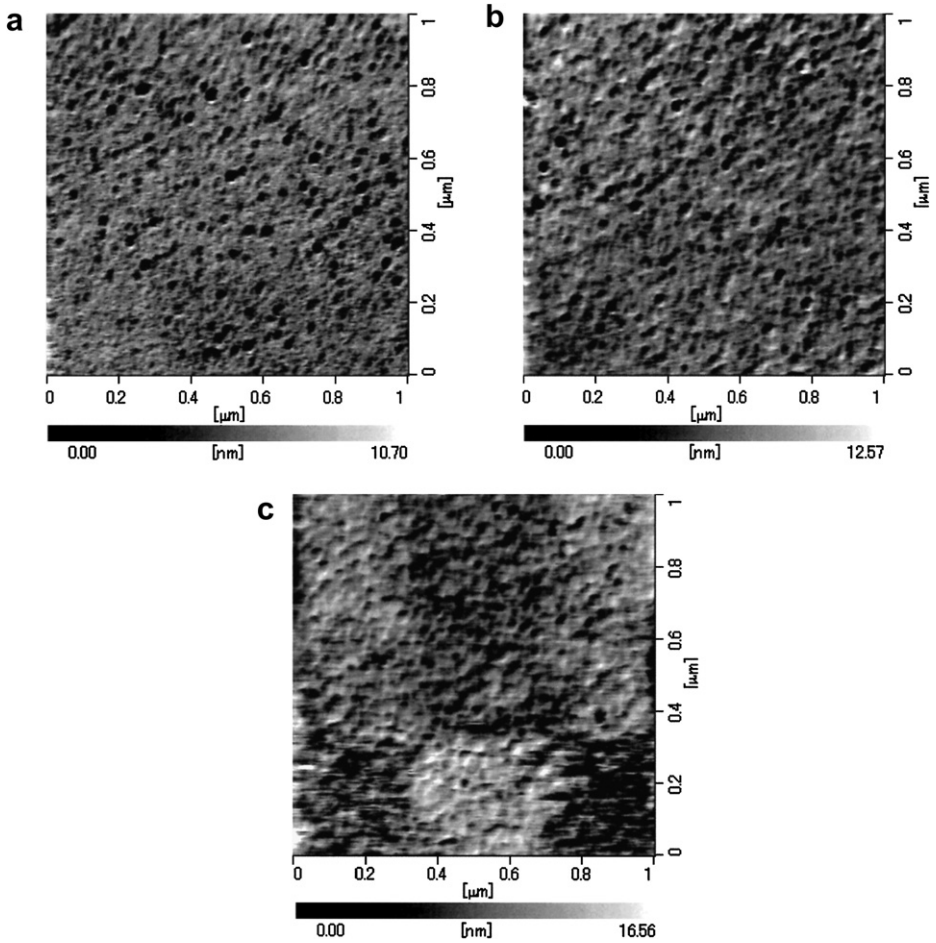

Fig. 4. (a–c). Two dimensional AFM images for nanocrystalline ZnO thin films deposited at 1.5, 2, and 3 J/cm^2.

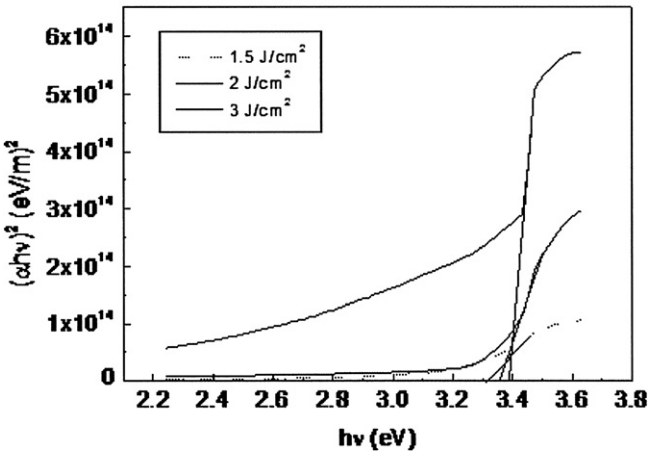

Fig. 6. Plot of $(\alpha h\nu)^2$ versus $h\nu$ for nanocrystalline ZnO thin films deposited at different laser energy density (1.5, 2 and 3 J/cm^2).

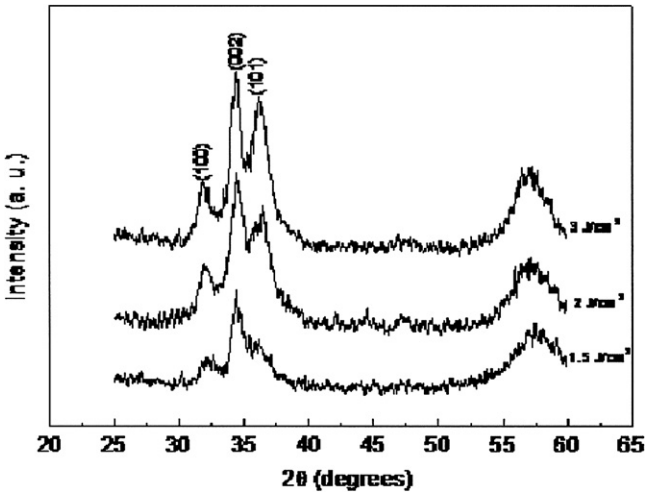

Fig. 7. X-ray diffraction patterns for nanocrystalline ZnO thin films deposited at 1.5, 2, and 3 J/cm^2.

different laser energy densities (1.5, 2 and 3 J/cm^2). Root-mean-square roughness and mean roughness of the deposited films are calculated and are given in Table 1. It shows that the root-mean-square roughness and mean roughness increases with an increase in laser energy density.

3.2. Optical properties

Fig. 5 shows the optical transmittance spectra of nanocrystalline ZnO thin films deposited using different laser energy densities. The absorption edge in transmittance spectra shifts towards the higher wavelength region. The blue shift in the transmittance spectra confirms that the optical band gap value increases with an increase in laser energy density. The relation between the absorption coefficient (α) and incident photon energy $h\nu$ can be written as [13]

$$\alpha h\nu = K_1\left(h\nu - E_g^d\right)^{\frac{1}{2}} \quad (1)$$

$$\alpha h\nu = K_2\left(h\nu - E_g^i\right)^2 \quad (2)$$

for direct allowed and indirect allowed transitions, where K_1 and K_2 are two constants. E_g^d and E_g^i are the direct and indirect band gaps, respectively. The graph between $(\alpha h\nu)^2$ versus $h\nu$ is shown in Fig. 6. Extrapolation of linear portion of the curve to $(\alpha h\nu)^2 = 0$ gives the optical band gap value of the deposited film. The deposited films show direct transition. The calculated optical band gap values are given in Table 1. It shows that the optical band gap value increases with an increase in laser energy density. The optical band gap value coincides well with the previous results for nanocrystalline ZnO films reported by Naszalyi et al. [14]. In Fig. 6, the low energy band tail confirms that the films deposited at 1.5 J/cm^2 have defects and impurities such as interstitial zinc atoms [15]. This is also confirmed in the composition analysis. The defects and impurity concentration decrease with an increase in laser energy density.

3.3. Structural properties

Fig. 7 shows the X-ray diffraction patterns of nanocrystalline ZnO films deposited at different laser energy densities (1.5, 2 and 3 J/cm^2). The X-ray diffraction patterns were obtained for 2θ values from 25° to 60°. The films deposited at different laser density show (002) preferred orientation. In addition, two more peaks (100) and (101), appear at 31.85 and 36.22^0, respectively. The peak intensity of (100) and (101) peaks increase with increasing laser energy density. For the film deposited at 1.5 J/cm^2 (002) a peak is observed at 34.427^0. Similar results have been reported by Rusop et al. [16]. The (002) peak position shifts towards high angle direction with an increase of laser energy density (Table 2). All the films prepared under these deposition conditions show strong c-axis (002) orientation growth. The (002) peak intensity also increases with the increase of laser energy density. This is attributed to the fact that the kinetic energy of the particles increases with increasing laser energy density. In other words, the particle size value increases with increase in laser energy density. XRD patterns show that the deposited films were crystallized in hexagonal phase and present a preferential orientation along the c-axis. The strain value can be calculated from the following relation

$$\varepsilon = \left[\frac{\lambda}{D\cos\theta} - \beta\right]\frac{1}{\tan\theta} \quad (3)$$

The dislocation density can be calculated from the following relation

$$\delta = \frac{1}{D^2} \quad (4)$$

Table 2
Structural parameters of nanocrystalline ZnO film deposited on silicon substrates.

Deposition parameters	2θ (degree)	Particle size (nm)	Strain × 10^{-3} (lin^{-2} m^4)	Dislocation density × 10^{15} lin/m^2	Lattice parameters (m)			Lattice spacing (m)
					A	*c*	*c*/*a*	
1.5 J/cm^2	34.4275	7.87	3.98	16.15	3.2486	5.2056	1.6024	2.6028
2 J/cm^2	34.4747	8.86	3.5298	12.74	3.2386	5.1988	1.6053	2.5994
3 J/cm^2	34.399	11.81	2.6487	7.1746	3.2486	5.2098	1.6031	2.6049

Lattice parameters a and c for the films deposited at 1.5 J/cm^2 are calculated as 3.2486 and 5.2056 Å ($c/a = 1.6024$), respectively. Calculated lattice parameters coincide well with other reported values [11]. The lattice spacing for the films deposited at 1.5 J/cm^2 is calculated as 2.6028×10^{-10}. The calculated lattice spacing value closely matched the reported values [16]. The calculated structural parameters are given in Table 2. This shows that the crystallite size increases with an increase in laser energy density, but the dislocation density decreases with increasing laser energy density.

4. Conclusion

Nanocrystalline ZnO thin films were deposited onto glass and silicon substrates using the PLD technique. XPS analysis was used to study the composition of the deposited film; it shows that the incorporation of oxygen into Zn is greatly increased at high laser energy density (3 J/cm^2). In optical studies, the blue shift in the transmittance spectra confirms that the optical band gap value increases with an increase in laser energy density. X-ray diffraction studies show the c-axis orientation of the deposited films.

References

[1] Luo Lei, Zhang Yanfeng, Mao Samuel S, Lin Liwei. Fabrication and characterization of ZnO nanowires based UV photodiodes. J Sens Actuators A 2006;127(2):201–6.
[2] Chang JF, Kuo HH, Leu IC, Hon MH. The effects of thickness and operation temperature on ZnO: Al thin film CO gas sensor. J Sens Actuators B 2002;84:258–64.
[3] Hauptmann P. Sensors principles and applications. Salisbury: U: Prentice Hall; 1991. p. 115–24.
[4] Wang Caihong, Chu Xiangfeng, Wu Mingmei. Detection of H_2S down to ppb levels at room temperature using sensors based on ZnO nanorods. J Sens Actuators B 2006;113:320–3.
[5] Si Shufeng, Li Chunhui, Wang Xun, Peng Qing, Li Yadong. Fe_2O_3/ZnO core–shell nanorods for gas sensors. J Sens Actuators B 2006;119:52–6.
[6] Zhang XT, Liu YC, Zhi ZZ, Zhang JY, Lu YM, Xu W, et al. High intense UV-luminescence of nanocrystalline ZnO thin films prepared by thermal oxidation of ZnS thin films. J Cryst Growth 2002;240:463–6.
[7] Zhang Yang, Lin Bixia, Fu Zhuxi, Liu Cihui, Han Wei. Strong ultraviolet emission and rectifying behavior of nanocrystalline ZnO films. J Opt Mater 2006;28:1192–6.
[8] Guo Min, Diao Peng, Cai Shengmin. Hydrothermal growth of perpendicularly oriented ZnO nanorod array film and its photo electro chemical properties. J Appl Surf Sci 2005;249:71–5.
[9] Leung CY, Djurisic AB, Leung YH, Ding L, Yang CL, Ge WK. Influence of the carrier gas on the luminescence of ZnO tetrapod nano wires. J Cryst Growth 2006;290:131–6.
[10] Vinay Gupta, Bhattacharya P, Yuzuk Yu I, Sreenivas K, Katiyar RS. Optical phonon modes in ZnO nanorods on Si prepared by pulsed laser deposition. J Cryst Growth 2006;287:39–43.
[11] Venkatachalam S. Kanno Yoshinori., Preparation and characterization of nano and micro crystalline ZnO thin films by PLD. Current Appl. Phys. 2009;9(6):1232.
[12] Chen M, Pei ZL, Wang X, Sun C, Wen LS. Structural, electrical, and optical properties of transparent conductive oxide ZnO: Al films prepared by dc magnetron reactive sputtering. J Vac Sci Technol 2001;19(3):963–70.
[13] Senadim Ebru, Eker Sitki, Kavak Hamide, Esen Ramazan. Optical and structural parameters of the ZnO thin film grown by pulsed filtered cathodic vacuum arc deposition. J Solid State Commun 2006;139:479–84.
[14] Naszalyi Livia, Deak Andras, Hild Elizabeth, Ayral Andre, Kovacs Attila L, Horvolgyi Z. Langmuir–Blodgett films composed of size-quantized ZnO nanoparticles: fabrication and optical characterization. J Thin Solid Films 2006;515(4):2587–95.
[15] Demiryont H, Nietering KE. Structure and optical properties of tin oxide films. J Sol Energy Mater 1989;19:79.
[16] Rusop M, Uma K, Soga T, Jimbo T. Post-growth annealing of zinc oxide thin films pulsed laser deposited under enhanced oxygen pressure on quartz and silicon substrates. J Mater Sci Eng B 2006;127:150–3.